NASA/TM–20250003674

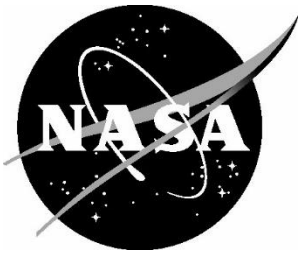

NASA Glenn Icing Research Tunnel: 2024 Cloud Calibration Procedure and Results

Emily N. Timko and Laura E. Hux
Amentum Technology, Inc., Cleveland, Ohio

Waldo J. Acosta
Glenn Research Center, Cleveland, Ohio

April 2025

NASA STI Program Report Series

Since its founding, NASA has been dedicated to the advancement of aeronautics and space science. The NASA scientific and technical information (STI) program plays a key part in helping NASA maintain this important role.

The NASA STI program operates under the auspices of the Agency Chief Information Officer. It collects, organizes, provides for archiving, and disseminates NASA's STI. The NASA STI program provides access to the NTRS Registered and its public interface, the NASA Technical Reports Server, thus providing one of the largest collections of aeronautical and space science STI in the world. Results are published in both non-NASA channels and by NASA in the NASA STI Report Series, which includes the following report types:

- TECHNICAL PUBLICATION. Reports of completed research or a major significant phase of research that present the results of NASA Programs and include extensive data or theoretical analysis. Includes compilations of significant scientific and technical data and information deemed to be of continuing reference value. NASA counterpart of peer-reviewed formal professional papers but has less stringent limitations on manuscript length and extent of graphic presentations.

- TECHNICAL MEMORANDUM. Scientific and technical findings that are preliminary or of specialized interest, e.g., quick release reports, working papers, and bibliographies that contain minimal annotation. Does not contain extensive analysis.

- CONTRACTOR REPORT. Scientific and technical findings by NASA-sponsored contractors and grantees.

- CONFERENCE PUBLICATION. Collected papers from scientific and technical conferences, symposia, seminars, or other meetings sponsored or co-sponsored by NASA.

- SPECIAL PUBLICATION. Scientific, technical, or historical information from NASA programs, projects, and missions, often concerned with subjects having substantial public interest.

- TECHNICAL TRANSLATION. English-language translations of foreign scientific and technical material pertinent to NASA's mission.

Specialized services also include organizing and publishing research results, distributing specialized research announcements and feeds, providing information desk and personal search support, and enabling data exchange services.

For more information about the NASA STI program, see the following:

- Access the NASA STI program home page at http://www.sti.nasa.gov

.

NASA/TM–20250003674

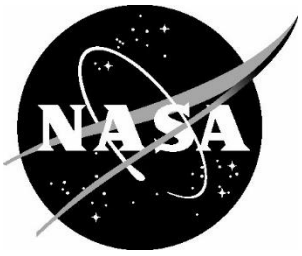

NASA Glenn Icing Research Tunnel: 2024 Cloud Calibration Procedure and Results

Emily N. Timko and Laura E. Hux
Amentum Technology, Inc., Cleveland, Ohio

Waldo J. Acosta
Glenn Research Center, Cleveland, Ohio

National Aeronautics and
Space Administration

Glenn Research Center
Cleveland, Ohio 44135

April 2025

Available from:

NASA STI Program / Mail Stop 050
NASA Langley Research Center
Hampton, VA 23681-2199

NASA Glenn Icing Research Tunnel: 2024 Cloud Calibration Procedure and Results

Emily N. Timko
Amentum Technology, Inc., Cleveland, Ohio

Laura E. Hux
Amentum Technology, Inc., Cleveland, Ohio

Waldo J. Acosta
Glenn Research Center, Cleveland, Ohio

Acknowledgements

The authors would like to thank NASA's Aerosciences Evaluation and Test Capabilities (AETC) Project for funding this cloud calibration effort. The Icing Research Tunnel (IRT) engineering staff also provided support with cloud calibration efforts and the authors would like to thank those individuals. The cloud calibration could not have been successful without the support, technical facility knowledge, and important work done by the IRT technician staff. In addition to the IRT staff, the authors would like to thank Science Engineering Associates, Inc. for the support with dropsizing probes and analysis.

Summary

The NASA Glenn Research Center 2024 Icing Research Tunnel cloud calibration results are presented in this report. The current status of the cloud uniformity, liquid water content, and dropsize calibration results will be discussed. The goals achieved in this calibration were to establish a uniform cloud and to generate transfer functions from the inputs of airspeed, spray bar atomizing air pressure, and spray bar water pressure to the outputs of median volumetric diameter (drop-size distributions) and liquid water content. This was completed for both Federal Aviation Administration (FAA) 14 CFR Parts 25 and 29, Appendix C and some Appendix O (supercooled large drop) conditions. The cloud uniformity from the Standard nozzles has remained the same as was reported for the 2019 full calibration. Changes were made to the Mod1 nozzle cloud to optimize uniformity while also maintaining water content values established in the 2019 full cloud calibration.

Nomenclature

CDP	Cloud Droplet Probe, drop sizer, 2 to 50 μm
DMT	Droplet Measurement Technologies
DOF	Depth of Field
$D_{v0.n}$	Drop diameter at which *n* percent of the total volume of water is contained in smaller drops
EAW	Effective Array Width
FAA	Federal Aviation Administration
FZDZ	Freezing Drizzle
FZRA	Freezing Rain
IRT	Icing Research Tunnel
K	Empirical function used in LWC curvefit
K_v	Function of velocity, used in LWC curvefit
K_a	Function of nozzle air pressure, used in LWC curvefit
LD	Large Drop conditions in the IRT: Mod1 nozzles, $2 \leq P_{air} \leq 8$ psig
LWC	Liquid Water Content, g/m^3
Mod1	Mod1 nozzles
MVD	Median Volumetric Diameter, μm
OAP–230X	Optical Array Probe, drop sizer, 15 to 450 μm
OAP–230Y	Optical Array Probe, drop sizer, 50 to 1,500 μm
P_{air}	Spray nozzle atomizing air pressure, psig
P_{water}	Spray nozzle water pressure, psig
RTD	Resistance Temperature Detector
SEA, Inc.	Science Engineering Associates, Inc.
SLD	Supercooled Large Drop
Std	Standard nozzles
TWC	Total Water Content, g/m^3
V	Calibrated true airspeed (velocity) in the test section, kn
ΔP	Spray nozzle $P_{water} - P_{air}$, psid

Introduction

The NASA Glenn Icing Research Tunnel (IRT) completed a full icing cloud calibration between September 2023 and June 2024 in accordance with the guidelines of SAE Aerospace Recommended Practice ARP5905, "Calibration and Acceptance of Icing Wind Tunnels" (Ref. 1). SAE ARP5905 recommends that a full calibration be performed five years following the previous full calibration. The last full calibration of the IRT cloud was completed in 2019 (Ref. 2). This report covers the procedures and results from the 2024 IRT full cloud calibration.

The steps taken to perform the calibration included establishing a uniform cloud and completing dropsize and liquid water content (LWC) calibrations for both Federal Aviation Administration (FAA) 14 CFR Parts 25 and 29, Appendix C and some Appendix O (supercooled large drop, SLD) conditions (Refs. 3 and 4). The first goal achieved of the calibration was to develop a uniform cloud for each nozzle set of the facility: Mod1 and Standard (Std) nozzles. Nozzle spraying locations were optimized; the number of spraying Mod1 nozzles changed from 103 in 2019 to 101 spraying nozzles and the Standard nozzle map remained the same at 165 spraying nozzles. Another goal was to generate transfer functions from the inputs of airspeed, spray bar atomizing air pressure, and spray bar water pressure to the outputs of median volumetric diameter (MVD) and LWC. New MVD and LWC curve fits for both the Mod1 and Standard nozzle sets were developed using the acquired data. The curves fit the data within ±10 percent for the Appendix C icing criteria and ±20 percent for the large drop icing conditions.

Facility Description

The IRT is a closed-loop refrigerated wind tunnel that simulates flight through an icing cloud. Figure 1 shows a plan view of the facility. A 5,000-hp (3,728.5-kW) motor drives the 25-ft- (7.6-m-) diameter fan with blades made of wood from Sitka spruce. The fan drives air through expanding turning vanes in C corner (see Figure 1) and into the face of the staggered 26-ft- (7.9-m-) high, 50-ft- (15.2-m-) wide heat exchanger. There, the air is chilled or warmed within a temperature range of 5 °C (41 °F) total to –40 °C (–40 °F) static. Twenty-four resistance temperature detectors, RTDs, are distributed on the D-corner contracting turning vanes and measure the total temperature in the settling chamber.

Downstream of the D-corner contracting turning vanes are ten spray bars with two different air atomizing nozzle types: Mod1 and Standard. The Mod1 nozzles have a lower water flow rate than the Standard nozzles. Each bar has 55 nozzle positions that contain either a Mod1 nozzle, a Standard nozzle, or a plug. The nozzle housings are connected to an air manifold and two water manifolds. The cloud (spray) is turned on using remotely controlled solenoid valves. The water manifolds can be individually turned on to spray only the Mod1 nozzles, only the Standard nozzles, or both (with the same atomizing air pressure). In 2006, vertically mounted struts were added to the spray bars. These struts were installed to improve the cloud uniformity and are still part of the system (Ref. 5).

The contraction area ratio into the test section is 14:1. The test section itself is 20 ft (6.1 m) long (axial) by 6 ft (1.8 m) high by 9 ft (2.7 m) wide. The center of the test section is 44 ft (13.4 m) from the spray bars. From the test section, the cloud flows into the diffuser toward A corner, into B corner, and into the fan. The calibrated speed range in the test section is from 25 to 300 kn.

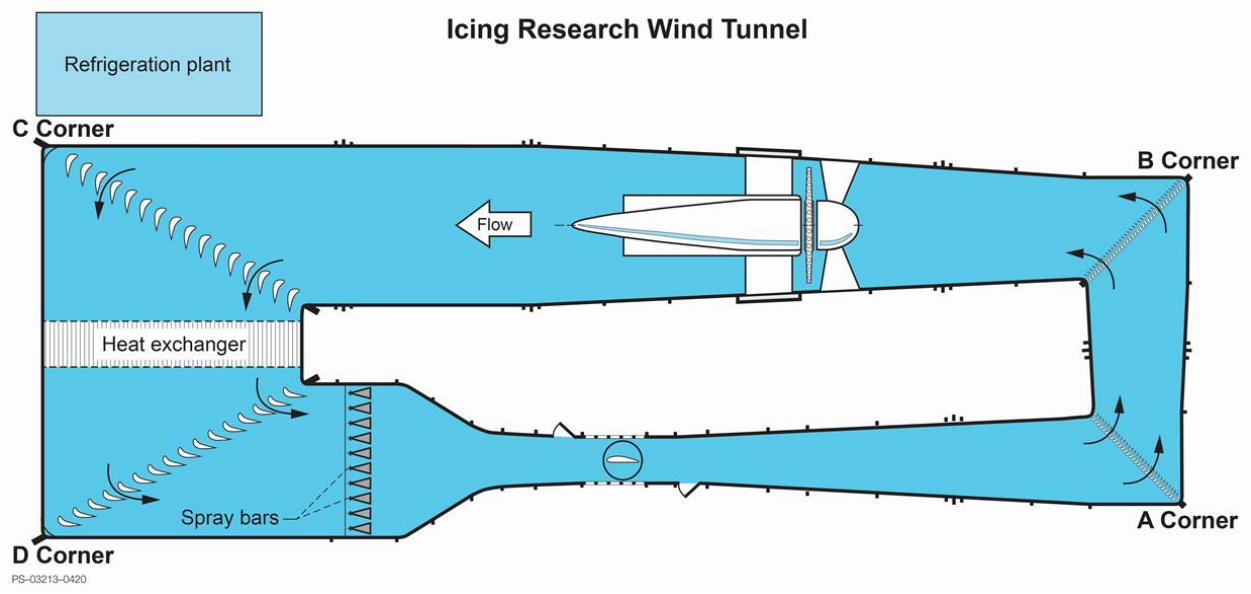

Figure 1.—NASA Glenn Research Center Icing Research Tunnel

Icing Cloud Uniformity

The first step in the calibration process was to establish a uniform cloud. This was done by optimizing a spray nozzle pattern that has the appropriate nozzles turned on or off for both the Mod1 and Standard nozzle sets to produce a uniform cloud.

Figure 2(a) shows the grid that was used to measure the cloud uniformity. The grid is 6 ft (1.8 m) high by 6 ft (1.8 m) wide and extends from the floor to the ceiling of the test section. The mesh elements are 2 in. (5.08 cm) deep with a flat 0.125-in. (0.3175-cm) face for ice accretion. Ice is accreted across the grid and then accretion thicknesses are measured on the vertical mesh elements, which are spaced every 6 in. (15.24 cm). Digital calipers are used to measure the ice thickness at the center point of the vertical elements. Figure 2(b) is an example of the accreted ice on the grid. The measured accretion values are then plotted as a ratio of the average of the central 12 values. Examples are shown in Figure 3. The light beige color shows that the LWC uniformity is within ±10 percent for most of the map.

(a)

(b)

Figure 2.— Cloud uniformity grid. (a) Grid mounted in center of test section in Icing Research Tunnel. (b) Ice accretion on grid elements.

A nozzle transfer map was established as a primary step in developing a uniform cloud. Single rows (i.e., spray bars) and columns of nozzles were sprayed to observe where ice accretes on the grid. This transfer map aids in the optimization of nozzle locations to produce a uniform cloud. Nozzle transfer maps can also be used as a tool to identify problematic nozzles during routine testing. In accordance with ARP5905 (Ref. 1), the IRT performed semiannual check calibrations between the 2019 full calibration and the 2024 full calibration. During this timeframe, there were no changes to the facility or the Standard or Mod1 nozzle spray patterns. From the check calibrations it was observed that the Standard nozzle cloud uniformity (created by 165 spraying nozzles) remained generally unchanged over the five years. Hence, in 2024, the Standard nozzle map was not altered, and it still contains 165 spraying nozzles. The

Mod1 cloud uniformity (created by 103 spraying nozzles) remained within ARP5905 recommendations but varying high and low spots would fluctuate toward the center of the map. Therefore, spraying nozzles located in the center of the nozzle map were adjusted to optimize the uniformity. This resulted in a change from 103 spraying nozzles to 101 spraying nozzles. The resulting cloud uniformity maps are shown in Figure 3(a) and (b) for Mod1 nozzles and Standard nozzles, respectively. These plots are viewed facing downstream. Uniformity for a large drop cloud which is produced using the Mod1 nozzles, MVD = 129 μm, is shown in Figure 3(c). The vertical extent of the cloud is smaller than those in the aforementioned figures. This is due to momentum of the large drops through the contraction that causes the trajectories to flow more toward the center.

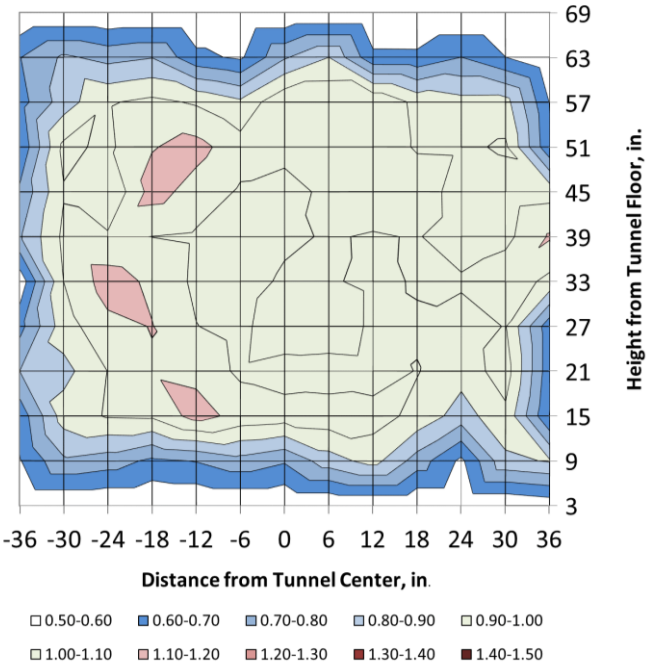

(a)

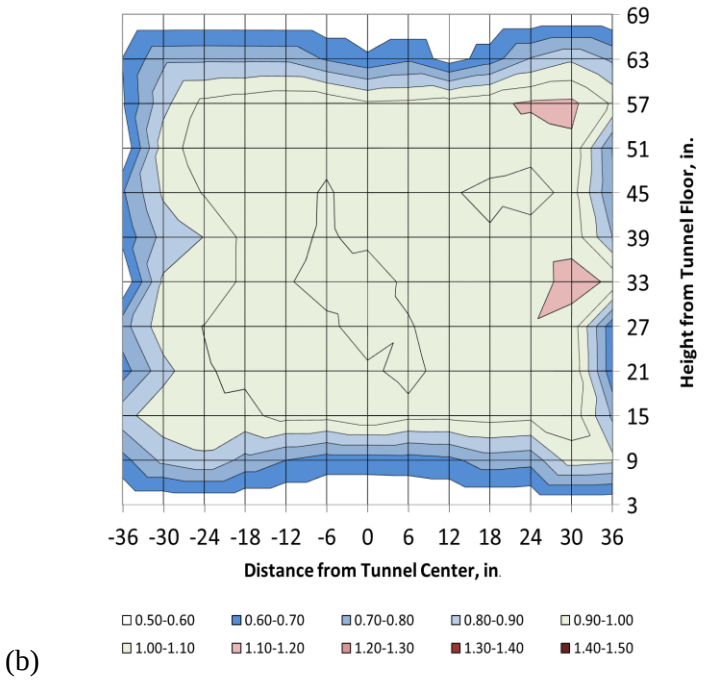

(b)

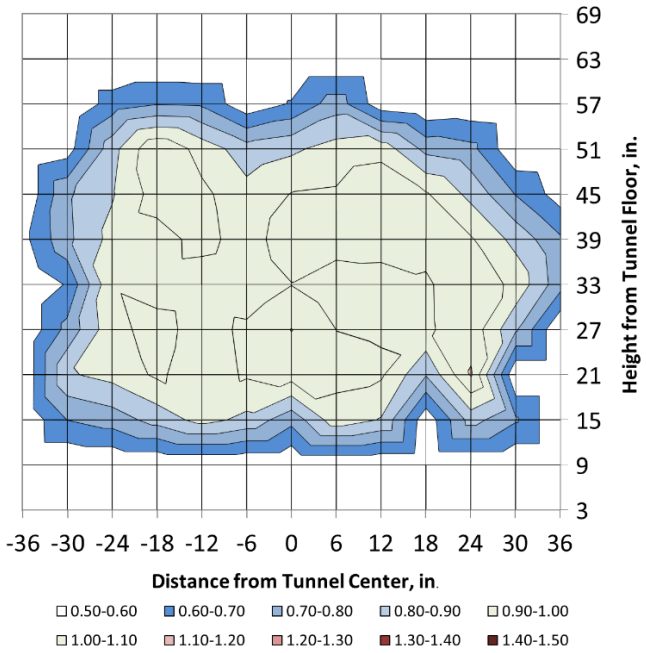

(c)

Figure 3.—Cloud uniformity viewed facing downstream, plotted as ratios to average accretion thickness from center 12 elements. (a) Mod1 nozzle cloud uniformity, 20-μm median volumetric diameter (MVD) at an airspeed of 150 kn. (b) Standard nozzle cloud uniformity, 20-μm MVD at an airspeed of 150 kn. (c) Large drop cloud uniformity, 129-μm MVD at an airspeed of 150 kn.

Drop-Size Calibration

Following the development of the cloud uniformity, a complete set of dropsize data was collected. In order to measure the full range of dropsizes in the IRT, three instruments were needed. For the 2024 dropsize calibration, the instruments used were the Cloud Droplet Probe (CDP) made by Droplet Measurement Technologies (DMT) and two Optical Array Probes (OAP–230X and OAP–230Y) made by Particle Measuring Systems. Figure 4 shows these probes mounted in the IRT test section.

The CDP measures dropsizes between 2 to 50 μm in diameter using the Mie-scattering theory for forward-scattered light intensity. When a drop passes through the beam path of the CDP laser, it scatters light in all directions and the forward-scattered light intensity is recorded by the probe and used to sort the dropsize into one of 30 size-bins or ranges. Since the CDP measures the smallest dropsizes of the three probes and since all spray conditions in the IRT contain small drops, data from the CDP is collected and used for the full range of spray conditions. The range of the spray conditions covered the following air pressures (P_{air}) and delta pressures (ΔP equals water pressure, P_{water}, minus P_{air} or $\Delta P = P_{water} - P_{air}$): for the nozzles, Mod1 are at $2 \leq P_{air} \leq 60$ psig and $5 \leq \Delta P \leq 250$ psid and Standard are at $10 \leq P_{air} \leq 60$ psig and $5 \leq \Delta P \leq 150$ psid.

The OAP–230X measures dropsizes between 15 to 450 μm and the OAP–230Y measures between the range of 50 to 1,500 μm. Both of the optical array probes measure dropsize using diode shadowing. An array of photodiodes is illuminated by a collimated laser beam and when a drop passes through the beam, the drop diameter is sorted into bins according to the number of diodes that are shadowed by more than 50 percent. At least one diode must be shadowed by 66 percent for the particle to be counted. Data were taken with the OAP–230X for all spray conditions that produce an MVD greater than 15 μm. The OAP–230Y usage was limited to larger drop conditions (spray conditions with nozzle air pressure < 10 psig). Drop-size distributions were determined by combining data from the CDP with the OAP–230X and OAP–230Y to calculate MVD.

(a) 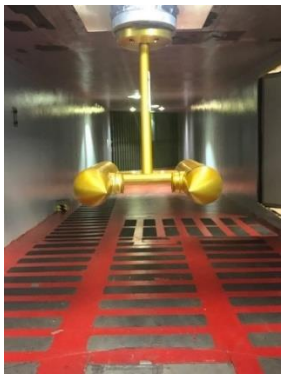 (b)  (c) 

Figure 4.—Three dropsizing instruments used for dropsize calibration mounted in Icing Research Tunnel test section. (a) Cloud Droplet Probe (CDP) by Droplet Measurement Technologies, 2 to 50 μm. (b) Optical Array Probe (OAP–230X), 15 to 450 μm and (c) Optical Array Probe (OAP–230Y), 50 to 1,500 μm are both made by Particle Measuring Systems.

Data Processing of Drop-Size Distributions

Spinning Disk Calibrations of DOF and Size for Optical Array Probes

Since the previous cloud calibration, there has been an improved understanding of the depth of field determination for the optical array probes. Prior to this development, the depth of field and defined bin widths that were used came from the instrument's operating manual.

Calibrations of the OAP-230X and OAP-230Y were performed by Science Engineering Associates, Inc., SEA, using spinning glass disks with dots of known diameters. The Depth of Field, DOF, is the ratio of the number of dots presented to the probe by the spinning disk during the traverse divided by the number of dots measured by the probe during the traverse. If any spots were not counted because they touched the edge of the array, the DOF value was reduced.

First, a cubic spline to fit the measured DOF values to the measured distance between the tips was used. Eventually, the DOF reached a maximum equal to the distance between the tips and a mathematical limit was applied once the spline's DOF exceeded the spacing between the arms.

The net sample area width is the product of the measured DOF times the Effective Array Width, EAW. The EAW is the probability that a drop of a given size will pass over the array without touching the edges of the array. Small drops have a high probability of crossing the array and not touching the edges, but their DOF is small. As the dropsize increases the DOF increases but at the same time the EAW decreases. At some point the DOF reaches the width of the arms and remains constant with increasing dropsize, but the EAW continues to decrease. This leads to a peak in the sample area, typically about one third of the way from the smallest to the largest drop.

The traverse method itself uses a spinning disk with multiple tracks, each with multiple dots of the same dot size, and a motor driven lead screw which moves the spinning disk from one arm through center to the other arm. A control system sets the rpm of the disk and controls the movement of the disk between the arms. Knowing the rpm of the disk and the diameter of the dot track, the effective spot velocity is known. Knowing the rpm and the number of spots on a given track, the number of dots presented to the probe in each amount of time is also known. The disk's position between the arms is known and the control system keeps the lateral velocity constant.

A traverse begins with the spinning disk at the one arm or the other. The traverse moves through center to the other extreme. The traverse rate is low compared to the number of dots being presented to the probe.

After the traverse, the number of dots counted by the probe is divided by the number of spots presented to the probe and multiplied by the total distance of the traverse. This gives the measured DOF.

DOF = length of traverse * sum(drops counted) / sum(drops presented)

During each traverse the instantaneous number of drops counted is multiplied by the average bin number observed. The overall average size for the traverse is the sum of the product of the counts times the bin number divided by the total number of counts.

Average bin size = sum (drops counted * bin number)/sum(drops counted)

The measured average bin size is then correlated to the known spot size on the spinning disk and these bin sizes were then used in data processing for the drop-size distributions. (Ref. 6)

Drop-Size Distributions

An example drop-size distribution is shown in Figure 5 combining all three probes for a large drop spray condition. The number density is the number of drops that are recorded in each bin normalized by the sample volume for that dropsize and the bin width. For Figure 5(a) and (b), the squares show the

size distribution as measured by the CDP, the triangles by the OAP–230X, and the circles by the OAP–230Y. The gray data points represent measurements from the respective probes that were not used in MVD calculation, as will be described in the following information. The volume is calculated using the median bin diameter size multiplied by the number of recorded counts, which then results in the LWC for each bin. Figure 5(b) shows an example LWC distribution for a case with an MVD of 253 μm where values are normalized by their respective bin widths. The MVD can then be determined by plotting the normalized cumulative water content versus drop diameter, as seen in Figure 5(c). Drop-size distributions are characterized by the MVD. This is the value at which half of the water volume is contained in smaller (or larger) drops. MVD can also be referred to as "$D_{v0.50}$". Correspondingly, $D_{v0.90}$ is the diameter at which 90 percent of the volume is contained in smaller drops. Normalized cumulative volume distributions for the IRT are shown in Figure 6. Bin volumes are plotted cumulatively, such that each data point represents the amount of water contained in all smaller diameters normalized by the total volume contained in all bins. Figure 6(a) shows cumulative volume distributions for MVD values less than or equal to 50 μm, and Figure 6(b) shows cumulative volume distributions for MVD greater than 50 μm.

As noted, the CDP, OAP–230X, and OAP–230Y each contribute measurements to the overall particle size distribution based on their sizing ranges. Their size ranges overlap, and efforts were made to determine how to address that overlap. Similarly to the 2019 full calibration, a cross over from the CDP to the OAP number densities at 46 μm, instead of 50 μm was used. More information can be found in Ref. 2 to support the crossover at 46 μm. Since the CDP otherwise shows good alignment with the OAP–230X measurements, the choice was made to use CDP data for diameters up to 46 μm and then use the OAP–230X data.

Because of the spinning disk calibration performed on the OAP probes, the bin definitions shifted and thus changed the crossover point from 367.5 μm for the 2019 full calibration data to 362 μm crossover from the OAP-230X to the OAP-230Y. Thus, the OAP–230X is used for particle sizes up to 362 μm and then crossover to use the OAP–230Y data if it were available. This diameter value was chosen because it was the most common value at which the OAP–230X was observed to deviate from the trend that was continued by the OAP–230Y as observed in Figure 5(b). Similar to the decision for CDP and OAP–230X crossover data, the uppermost bins from the OAP–230X were not used if there was OAP–230Y data that could be used instead. This is because the OAP–230Y showed good agreement with the overall trend of the distribution, while the uppermost bins of the OAP–230X appear to be undercounting, as can be seen by the gray triangles in Figure 5(b). Both OAPs only return one-dimensional (1D) data, and if a particle shadows either end (qualifier) diode, it is not sized, and thus it becomes statistically difficult for particles at the upper end of the probe's range to pass through the middle of the sizing array. Hence, these particles may be undercounted. It should be noted that for both the CDP and OAP–230X, these issues become more pronounced as MVD increased, and it was not generally necessary to discard probe data at these values if no larger range data was taken.

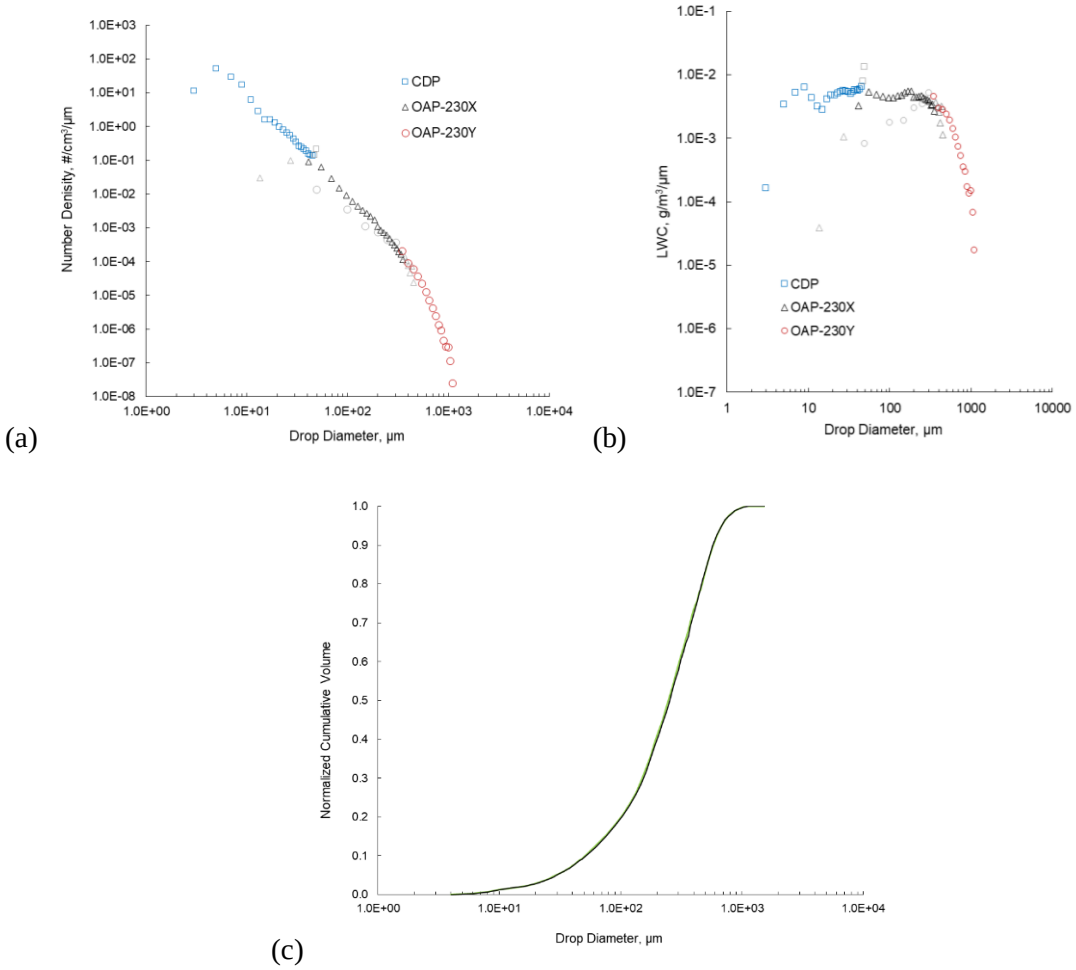

Figure 5.—Drop-size distribution combining all three probes for median volumetric diameter (MVD)=253 µm. All go into calculations for MVD. Gray data points represent measurements from respective probes that were not used in MVD calculation. (a) Number density distribution. (b) LWC distribution. (c) Cumulative volume distribution.

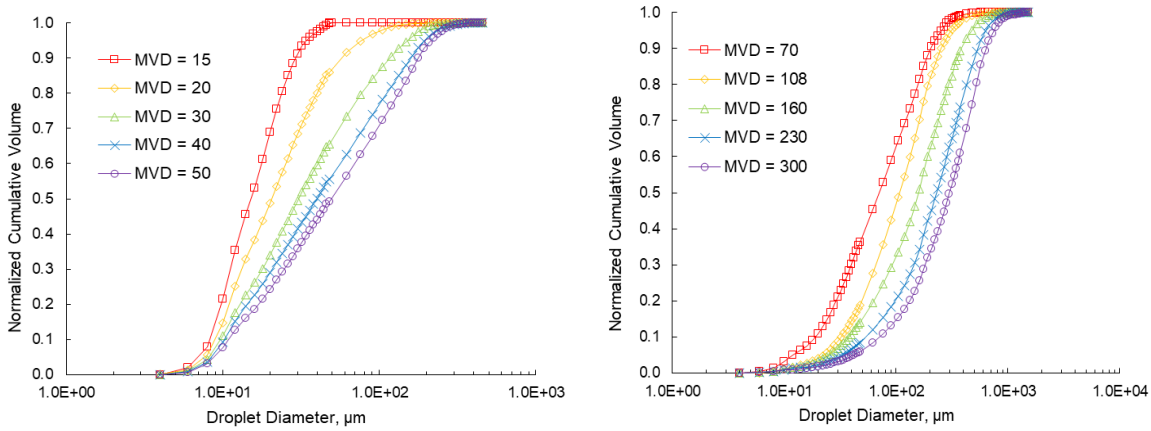

(a) (b)

Figure 6. –Normalized cumulative volume plots for two Icing Research Tunnel dropsize regimes. (a) Size range 15 to 50 μm. (b) Size range >50 μm up to maximum calibrated.

Dropsize Equations

The purpose of the dropsize calibration is not only to determine drop-size distributions but also to develop curve-fit equations. The equations developed have an input of measured atomizing P_{air} and ΔP ($P_{water} - P_{air}$). The curve fit generator, TableCurve (Systat Software, Inc.) was used to generate an appropriate equation that fit the majority of the data within ±10 percent.

The Mod1 MVD curve fit equation is

$$MVD_{Mod1} = a + b * {P_{air}}^{c} + d * \Delta P^{e} + f * {P_{air}}^{c} * \Delta P^{e} \quad (1)$$

where a = 12.625692, b = -151.23557, c = –2.6903876, d = 0.0000251981, e = 1.8175885, and f = 14.307142.

And the Standard MVD curve fit equation is

$$MVD_{Standards} = a + b\left[\frac{1}{1+\left(\frac{P_{air}}{c}\right)^{-d}}\right] + e\left[\frac{1}{1+\left(\frac{\Delta P}{f}\right)^{-g}}\right] + h\left[\frac{1}{1+\left(\frac{P_{air}}{c}\right)^{-d}}\right] * \left[\frac{1}{1+\left(\frac{\Delta P}{f}\right)^{-g}}\right] \quad (2)$$

where a = 17.591151, b = –3.4173098, c = 8.7596588, d = 3.6912316, e = 63766.874, f = 179.87013, g = 2.7929574, and h = –63765.636.

Figure 7(a) and (b) summarize these curve fits for Mod1 and Standard nozzles, respectively. In Figure 7, the curve fit lines are plotted as a function of ΔP for each calibrated P_{air} line. Figure 8(a) and (b) show how the curve fit values from the generated equations compare to the measured values for all Mod1 and Standard conditions, respectively. These plots show that the curve fits for the data points are within in the IRT's typical targeted accuracy of ±10 percent for the Appendix C cloud.

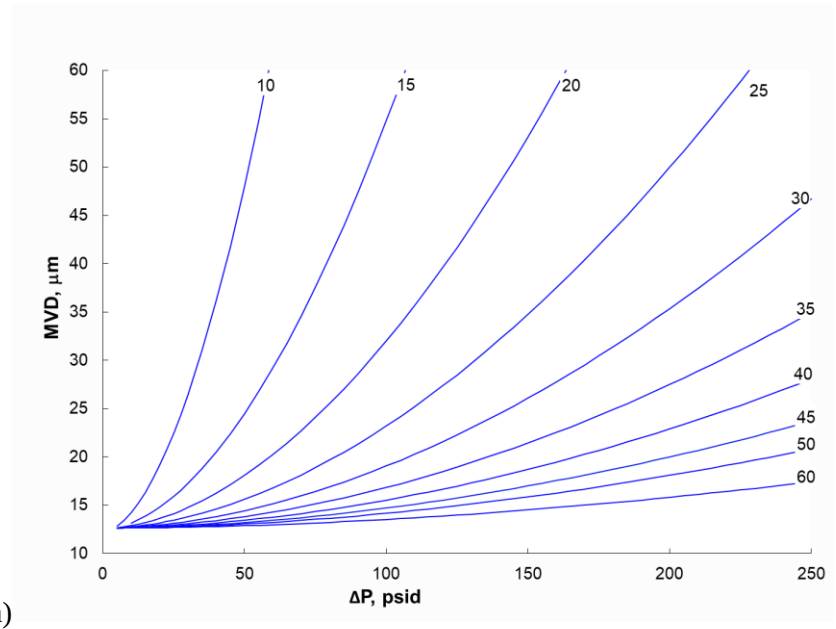

(a)

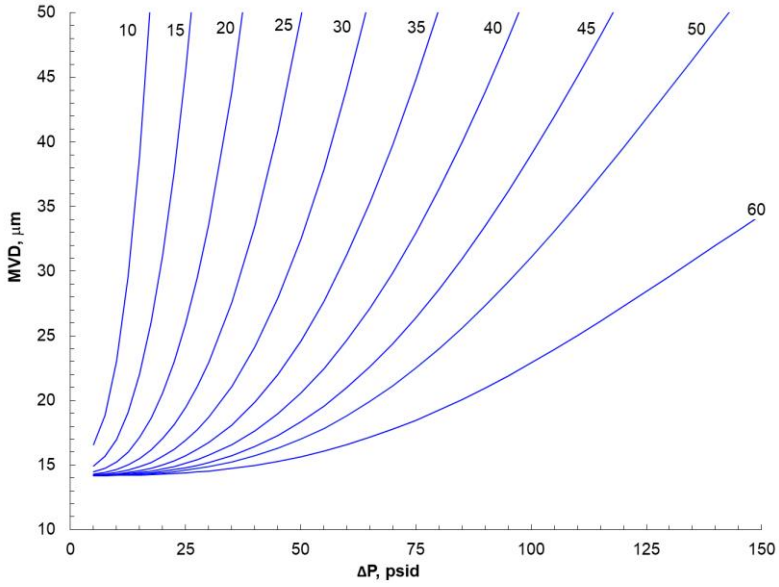

(b)

Figure 7.—Median volumetric diameter (MVD) curve fits as function of ΔP for each atomizing air pressure (P_{air}). (a) Mod1 nozzles (b) Standard nozzles

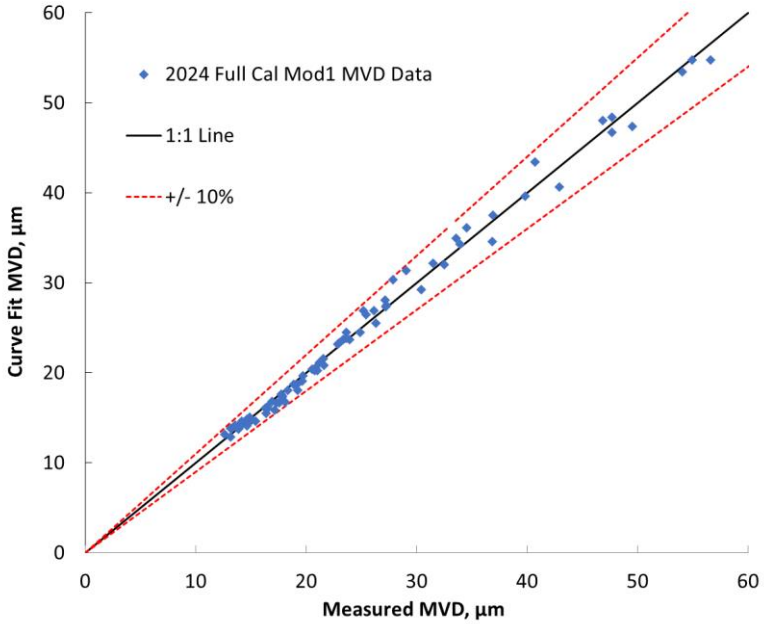

(a)

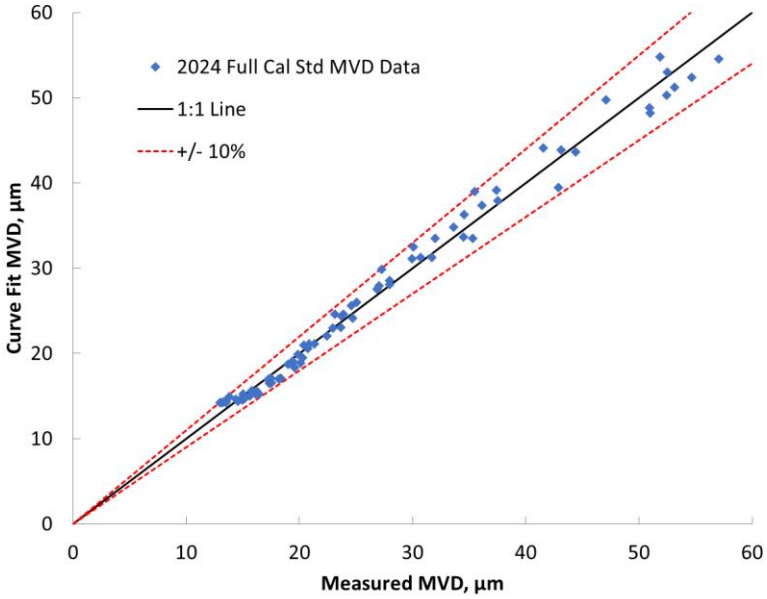

(b)

Figure 8.—Curve fit Median Volumetric Diameter (MVD) values from generated equations compared to measured MVD values for Federal Aviation Administration (FAA) 14 CFR Parts 25 and 29, Appendix C conditions. (a) Mod1 nozzles (b) Standard nozzles

Large Drops in the Icing Research Tunnel

A third equation was generated for larger drops (Appendix O). Large drops are achievable by reducing the spray nozzle atomizing air pressure so there is less breakup of the water stream. Operating

the Mod1 nozzles between $2 \leq P_{air} \leq 8$ psig is referred to as large drop conditions in the IRT, often abbreviated as LD.

The drop-size distributions for large drop conditions were measured by combining data from the CDP, OAP–230X, and OAP–230Y. The large drop curve fit equation is

$$MVD_{LD} = a + b * P_{air} + c * \ln(\Delta P) + d * {P_{air}}^2 + e * [\ln(\Delta P)]^2 + f * P_{air} * \ln(\Delta P) + g * {P_{air}}^3 + h * [\ln(\Delta P)]^3 + i * P_{air} * [\ln(\Delta P)]^2 + j * P_{air} * [\ln(\Delta P)] \quad (3)$$

where a = 217.70797, b = –46.4291, c = -89.980441, d = 27.790465, e = 71.325008, f = –66.74884, g = –1.4536626, h = -2.8849779, i = 4.5184991, and j = 0.6597944.

Figure 9 summarizes the MVD curve fits for the large drop operating range. Figure 9(a) shows the curve fit lines as a function of ΔP for each P_{air} line. Figure 9(b) shows the MVD goodness of fit, plotting how the curve fit values compare to the measured MVD. For large drop criteria, the IRT was able to fit the data to a curve within ±20 percent, shown in the figure as well. Comparisons of the IRT distributions to the FAA Appendix O (Ref. 4) requirements are shown in Figure 10 for both Freezing Drizzle (FZDZ) and Freezing Rain (FZRA) conditions. For FZDZ, MVD < 40 μm (Figure 10(a)) and FZDZ, MVD > 40 μm (Figure 10(b)), IRT distributions are selected that match the MVD (Dv0.5), or Dv0.98. Matching Dv0.98 (or similarly, Dv0.95 or 0.90) rather than the MVD would better assure that the effects of the larger drops in the distribution are captured. In Figure 10(c), there are two IRT distributions showing the relationship to the Dv0.5 and Dv 0.98 FAA Appendix O distribution for FZRA MVD < 40 μm.

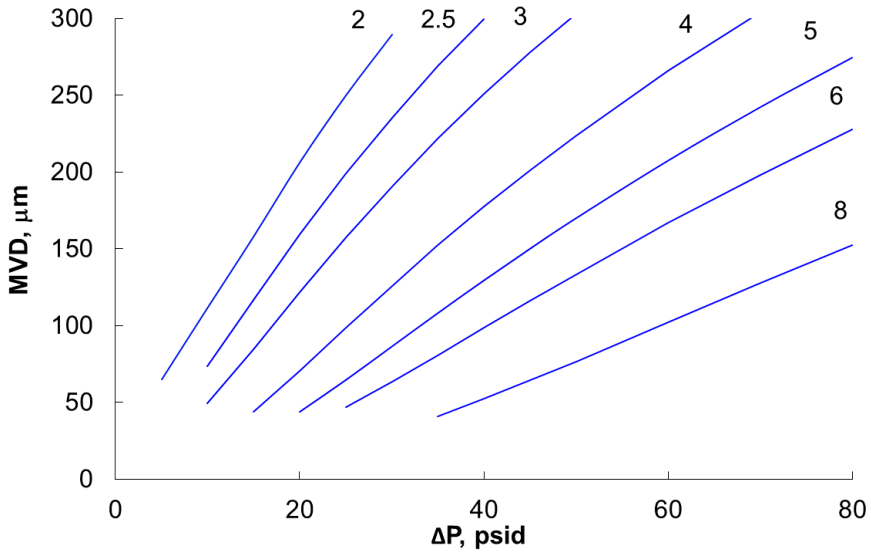

(a)

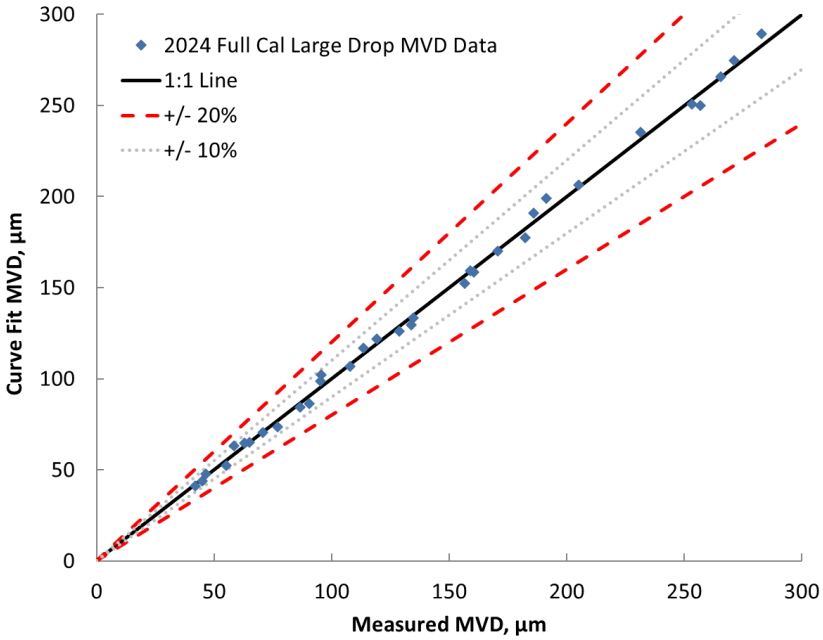

(b)

Figure 9.—Curve fit values from the generated equations compared to the measure values for Federal Aviation Administration (FAA) 14 CFR Parts 25 and 29, Appendix O conditions. (a) Median volumetric diameter (MVD) curve fits for large drop as a function of ΔP for each atomizing air pressure (Pair). (b) Curve fit compared to measured values for large drop conditions.

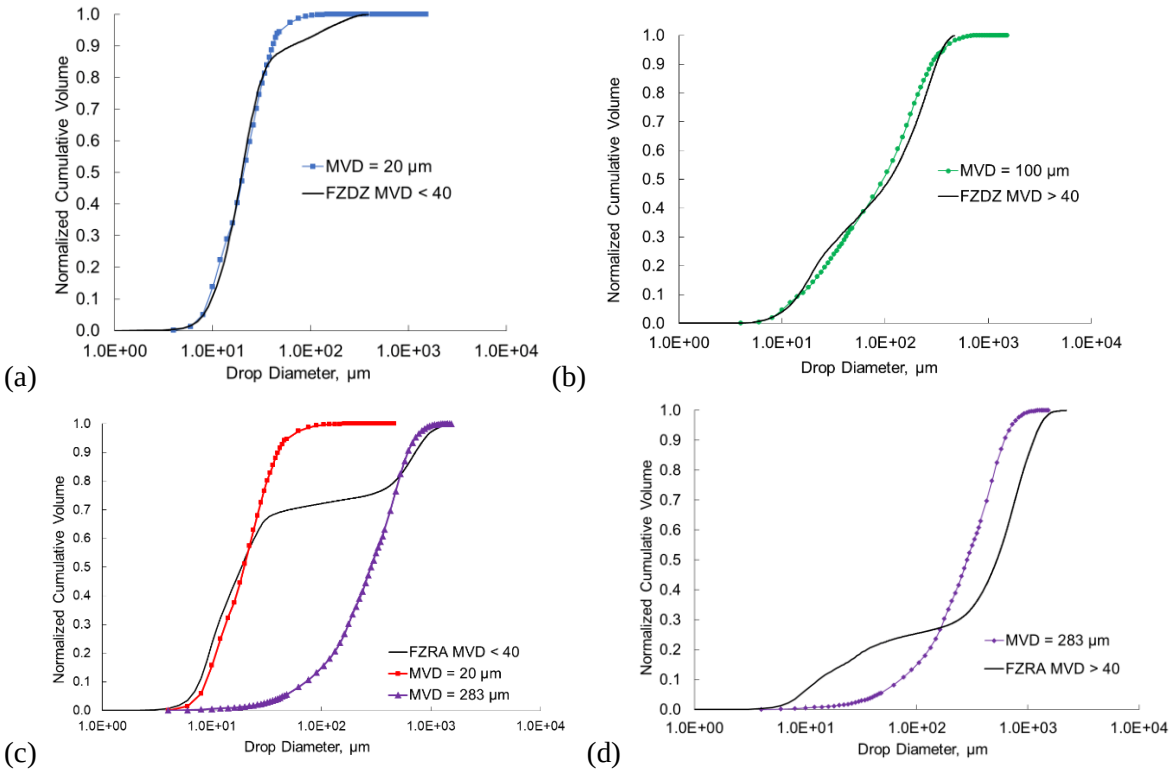

Figure 10.—Icing Research Tunnel (IRT) distributions to Federal Aviation Administration (FAA) 14 CFR Parts 25 and 29, Appendix O requirements for both Freezing Drizzle (FZDZ) and Freezing Rain (FZRA) conditions. (a) FZDZ, median volumetric diameter (MVD) <40 µm. (b) FZDZ, MVD >40 µm. (c) FZRA, MVD <40 µm. (d) FZRA, MVD >40 µm.

Liquid Water Content Calibration

The Multi-Element Sensor (commonly known as the multi-wire) manufactured by Science Engineering Associates, Inc. (SEA, Inc.), was used to measure cloud LWC. Pictures of this instrument are shown in Figures 11 and 12. The sensing elements are positioned inside a heated shroud that is approximately 1 in. (25.4 mm) in diameter. A typical multi-element shroud contains three sensing elements of various sizes, as well as a compensation wire. The elements, shown in greatest detail in Figure 11(b), are a 0.083-in.- (2.1-mm-) diameter hollow cylinder, 0.083-in.- (2.1-mm-) diameter forward-facing half-pipe (total water content or TWC) element, and a 0.021-in.- (0.5-mm-) diameter wire. A compensation wire is located behind the central element, parallel to the shroud. The compensation wire is designed to compensate for changes in atmospheric conditions, for example, temperature and pressure. It is intended to stay dry. Newer multi-element sensors employ a 0.083-in.- (2.1-mm-) diameter rear-facing half-pipe element in place of the hollow cylinder element. Greater details on the theory of operation of the instrument can be found in References 8 and 9.

Though the multi-wire has been used as the primary instrument to calibrate the IRT LWC since 2011, the 2024 multi-wire data was validated against measurements from an icing blade (hereon referred to as “the blade”) that had previously been used to calibrate LWC in the IRT until 2011. The blade is an accretion-based instrument with dimensions of 0.125 in. (3.18 mm) wide by 6.06 in. (154-mm) long by 0.75 in. (19.05 mm) thick. It is mounted in such a way that it is located at the horizontal centerline and the vertical center of the test section. It is run at a tunnel total air temperature between –0.4 and –4 °F (–18

and –20 °C) in an attempt to ensure that rime ice is accreted on the 0.125-in. (3.18-mm) flat face in most cases. Prior to use of the multi-wire as the primary instrument, the blade was the main LWC instrument of the IRT before 2011. It is described in detail in References 1 and 9.

Based on the results from Reference 9, further testing was done in 2016 to compare different mounts for the multi-wire. Particular focus was given to the measured water content values for the different conditions and configurations and how well they compared with blade measurements for low impingement conditions (i.e., below the Ludlam limit for the blade). Tests were completed for both the Mod1 and Standard nozzle sets across the IRT's full range of airspeeds, MVDs, and nozzle air pressures. To confirm the accuracy of LWC measurements, several data points were taken in 2024 with the icing blade for conditions below the blade's Ludlam limit, and these were compared to measurements with the multiwire. Test conditions included velocities from 50 to 300 kn, MVD values from 15 to 50 μm, and nozzle air pressure values from 10 to 60 psig, all expected to be below the blade's Ludlam limit. The multi-wire data in this plot has been corrected for collision efficiency, as will be described in the following information.

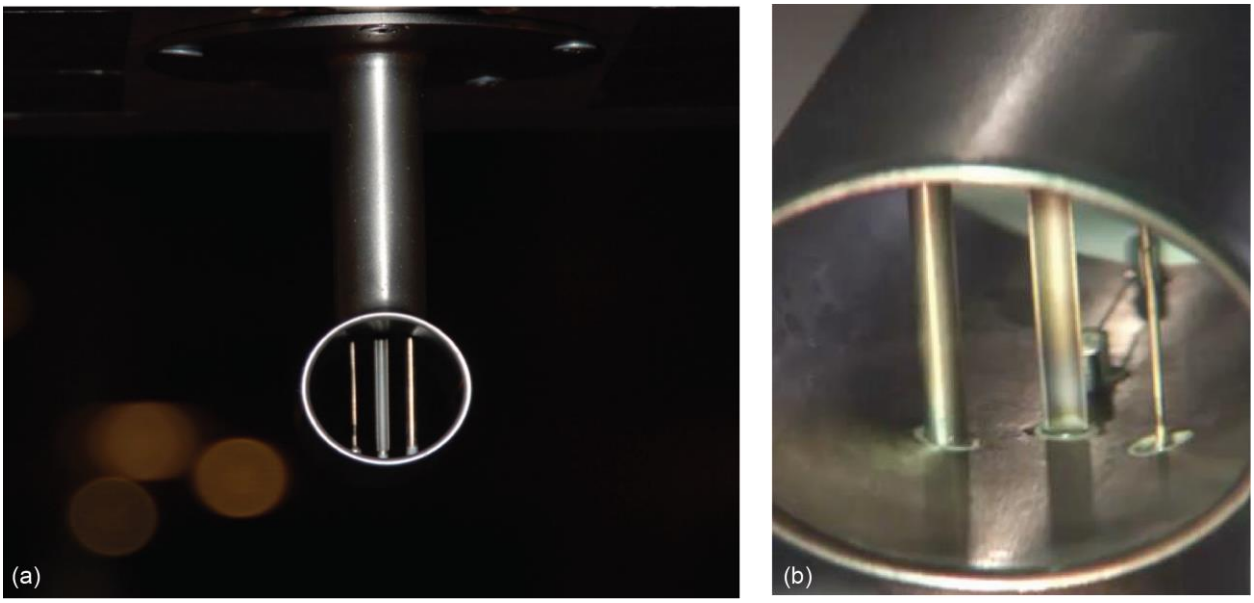

Figure 11.—Science Engineering Associates, Inc., Multi-Element Sensor. (a) Closeup view. (b) View of elements rotated 180° from (a).

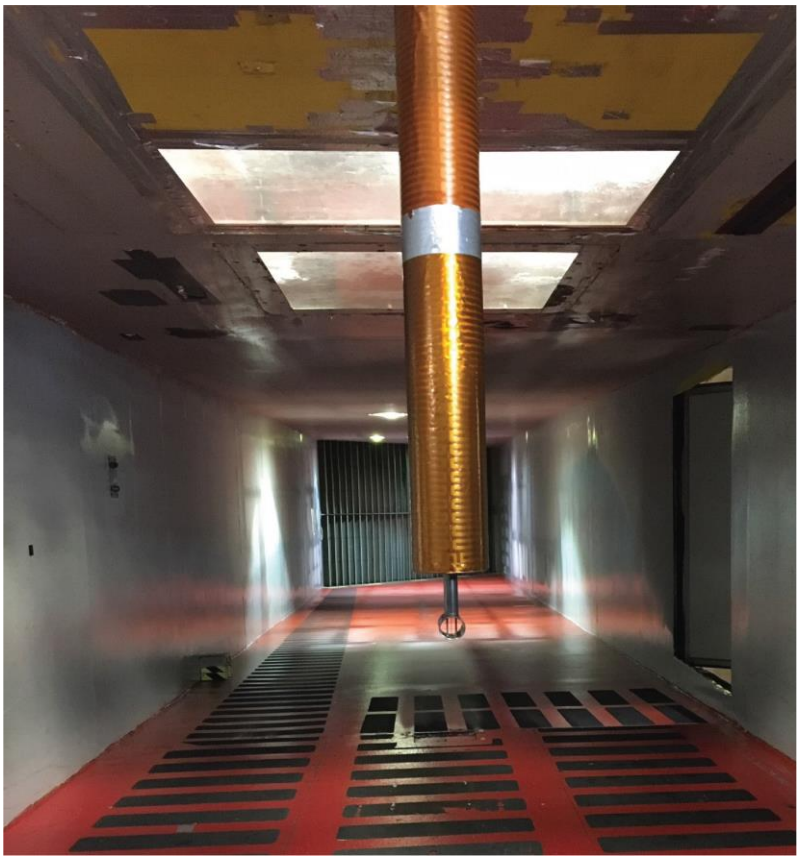

Figure 12.—Multi-Element Sensor (Science Engineering Associates, Inc.) mounted in the test section.

The IRT uses SEA Inc.'s M300 Data Acquisition System along with their WCM–2000 system to collect data from the multi-element sensor. The M300 records the power output of each of the sensing elements and receives the facility conditions from the facility control system, including total temperature, static temperature, airspeed, static air pressure, spray bar nozzle pressures, and whether the spray is on or off. All necessary calibration values and sensing element dimensions are received from the probe, and these are used along with the received facility conditions such that the data system can correlate the power of each sensing element to a calculated LWC. All the recorded values are output as 1-second averages into a CSV file. Once the data has been retrieved from the M300, it is postprocessed using a MATLAB® (The MathWorks, Inc.) code that was developed in-house. This code averages the data system outputs for each spray, starting 20 s after the spray begins and ending 2 s before the spray ends. A plot is generated for each spray so that the user may view the profile of the data and decide if the data seem reasonable. Further details can be found in Reference 9.

The smallest drops in the cloud are diverted around the sensing elements rather than impinging, particularly at low speeds, and so the measured LWC must also be corrected for the sensor's collision efficiency (also frequently called the collection efficiency). The primary sensor element used for LWC measurements in the IRT is the 2.1-mm-diameter forward-facing half pipe. In 2014, Rigby, Struk, and Bidwell (Ref. 10) modeled this sensing element along with the other two inside the multi-element sensor shroud using LEWICE3D, a particle trajectory code coupled with a three-dimensional (3D) flow-field analysis. They determined the correlation between the drop collision efficiency and the modified inertia parameter for drop diameters of 5, 20, 50, and 100 μm (Ref. 10). Struk then used this correlation to find total collision efficiency values based on particle size distributions measured in the IRT, rather than monodisperse drops (Ref. 11, personal communication). These values were in turn used to develop a formula for the collision efficiency correction as a function of MVD and airspeed in the IRT. Using this

equation, collision efficiency corrections are applied to all data from the multi-element sensor to determine the actual cloud LWC based on the measured values. All the data in this report have been adjusted with the collision efficiency correction based on the 3D geometry and the particle size distribution that was just described. This correction is only 1 to 2 percent for dropsizes larger than 100 μm at airspeeds above 100 kn, but the correction increases as dropsize and airspeed decrease. The water content may be as much as 10 percent higher than measured for a drop-size distribution with an MVD of 20 μm at 100 kn. For a drop-size distribution with an MVD of 15 μm at 50 kn, the correction is greater than 15 percent.

The data from the TWC or half-pipe element of the multiwire were corrected for collision efficiency according to the test point's particle size distribution and then compiled to build the LWC curve fits, correlating LWC to P_{air}, ΔP, and V. As described in the 2006 IRT calibration report (Ref. 5), the LWC calibration is a function of the form:

$$LWC = K(V, P_{\text{air}})\frac{\sqrt{\Delta P}}{V} \tag{4}$$

where K is a function of V and P_{air}. Fitting the LWC curve involves determining the function K for both parameters, Ka and Kv. To define Kv, measurements were made from V = 50 to 300 kn while P_{air} and ΔP (and MVD) are held constant. Similarly, to determine Ka, V and MVD were held constant while making measurements from P_{air} = 10 to 60 psig. K is calculated for each of the measured values by rearranging Equation 4: $K = LWC * \frac{V}{\sqrt{\Delta P}}\frac{V}{\sqrt{\Delta P}}\frac{V}{\sqrt{\Delta P}}$. Once relationships are found, they are combined to determine the surface function, K, which is unique for the Mod1 and Standard nozzle sets, as well as the LD conditions. In previous years, this relationship was linear but in 2019 and again in 2024, a polynomial relationship was found. Equations 5, 6, and 7 are the respective equations for each.

$$LWC_{Mod1} = \left(a + b * V^2 + c * V + d * {P_{\text{air}}}^2 + e * P_{\text{air}}\right) * \frac{\sqrt{\Delta P}}{V} * \left(\frac{MVD - f}{g}\right)^h \tag{5}$$

where a = 10.91, b = –0.00005, c = 0.0637, d = 0.0008, e = –0.1316, f = 4.6, g = 23.6, and h = 0.12.

$$LWC_{\text{Standards}} = (a + b * V^2 + c * V + d * P_{\text{air}}) * \frac{\sqrt{\Delta P - e}}{V} * \left(\frac{MVD - f}{g}\right)^h \tag{6}$$

where a = 41.75, b = –0.0004, c = 0.2566, d = –0.29, e = 1.4, f = 4, g = 23, and h = 0.05.

$$LWC_{LD} = \left(a + b * V^2 + c * V + d * {P_{\text{air}}}^2 + e * P_{\text{air}}\right) * \frac{\sqrt{\Delta P - f}}{V} * \left(\frac{MVD}{g}\right)^h \tag{7}$$

where a = 14.4311, b = –0.0001, c = 0.0773, d = –0.148, e = 0.9293, f = 1, g = 135, and h = 0.155.

Figure 13(a) and (b) show the goodness of fit of the LWC equations for the Mod1 and Standard nozzle sets, respectively. These reference lines show that the curve fits agree with the majority of the data within ±10 percent, which is the target accuracy of the IRT. The LD conditions have a target accuracy of ±20 percent but as seen in Figure 13(c), the LWC curve fit agrees with majority of the data within ±10 percent for LD conditions.

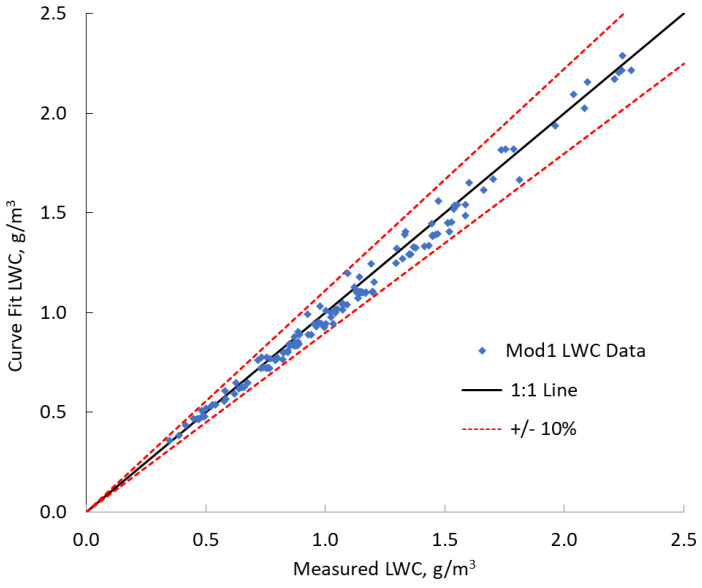

(a)

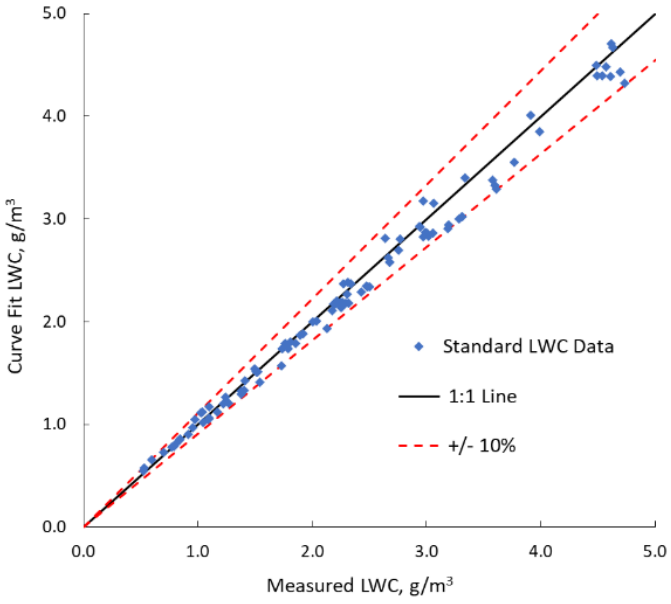

(b)

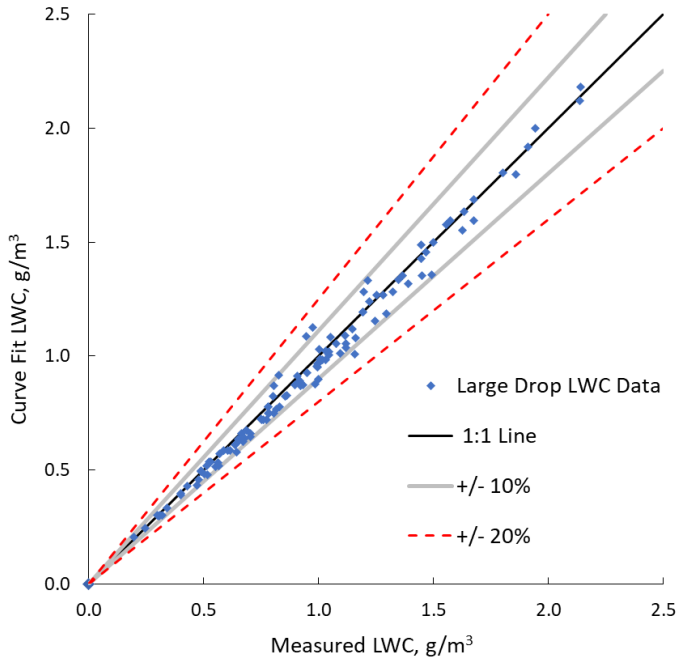

(c)

Figure 13.—Curve fit values from generated equations compared to measured values. (a) Mod1 nozzle set. (b) Standard nozzle set. (c) Large drop conditions. Liquid water content (LWC).

Icing Cloud Operating Envelopes

The IRT's icing envelopes for both the Mod1 and Standard nozzles are compared to the FAA Appendix C icing criteria (Ref. 3) in Figure 14 for an airspeed of 225 kn. The operating envelopes for LD conditions (Mod1 nozzles, $P_{air} \leq 8$ psig) are shown in Figure 15. Cloud LWC is airspeed dependent; at higher airspeeds, lower LWC values can be reached, and conversely so for lower airspeeds. This is demonstrated in Figure 15(a) and (b). It should be noted that LD conditions are only calibrated for airspeeds between 100 to 250 kn, unlike Appendix C conditions, which are calibrated for airspeeds between 50 to 300 kn. Additionally, MVD and LWC uncertainty for LD conditions is ±20 percent rather than ±10 percent for Appendix C. Cloud size also tends to be smaller, and uniformity might not be as good, depending on the test condition, as can be seen from comparing Figure 3(a) and (c).

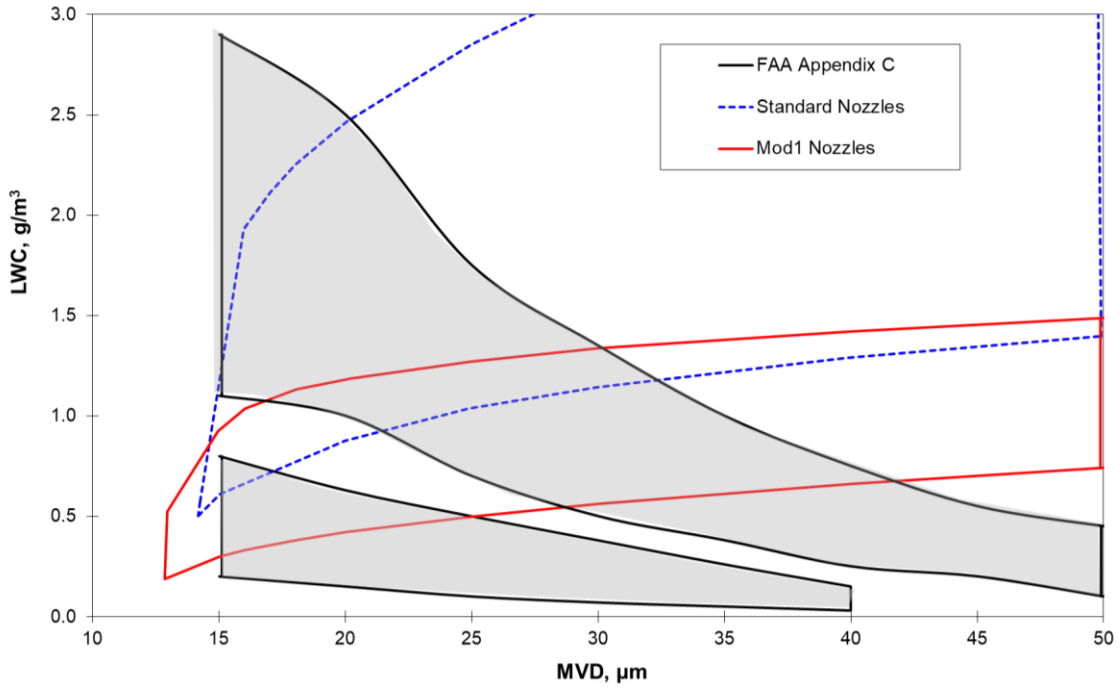

Figure 14. – 2024 Icing Research Tunnel operating envelopes for airspeed of 225 kn with median volumetric diameter (MVD)<50 µm compared against Federal Aviation Administration (FAA) 14 CFR Parts 25 and 29, Appendix C envelopes.

The operating envelopes for the large drop conditions are shown in Figure 15(a) and (b), which also show the inversely proportional airspeed and LWC relationship. These two plots also indicate the FZDZ and FZRA conditions as specified by the FAA in Reference 4, according to their MVD values and LWC ranges. Those who wish to test FAA Appendix O conditions in the IRT may contact any of the authors of this report to discuss options.

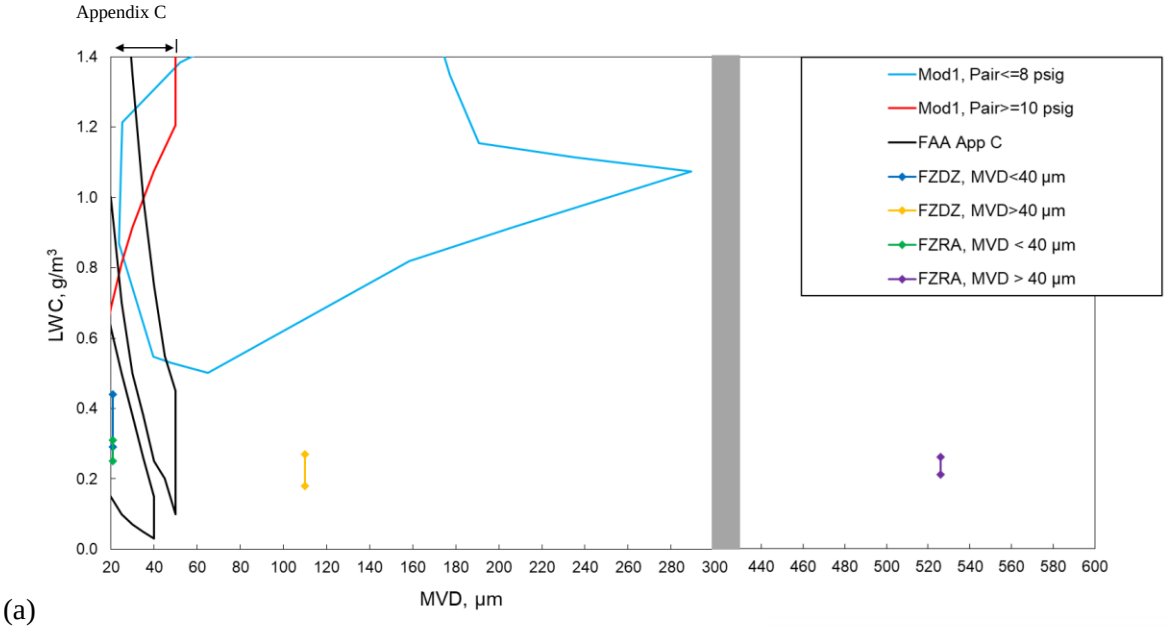

(a)

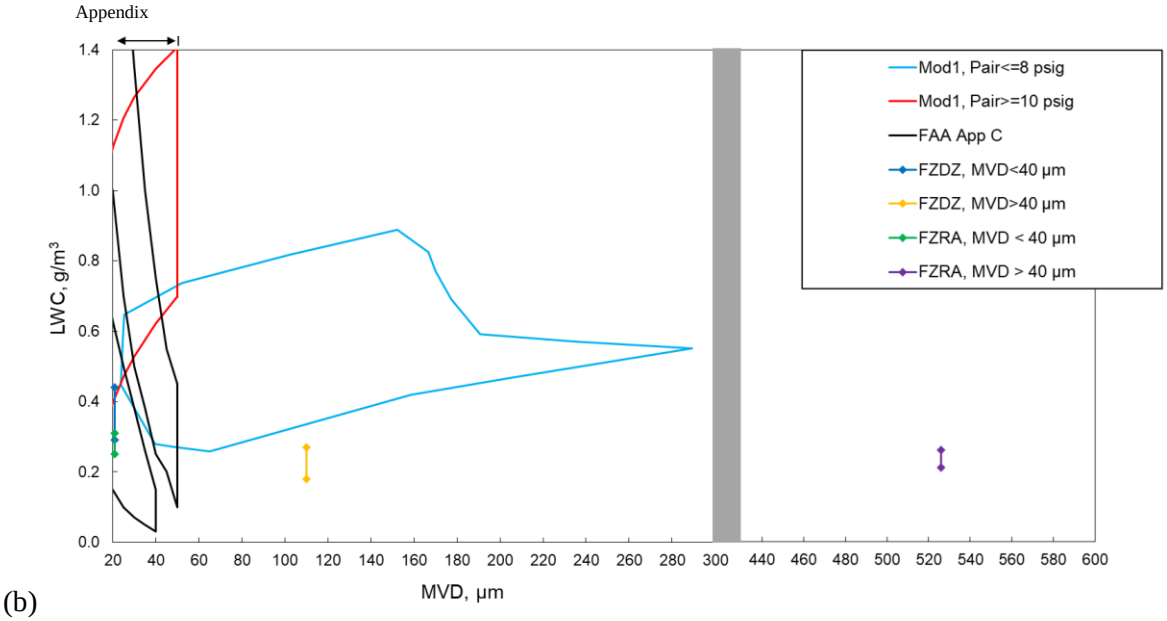

(b)

Figure 15. – 2024 Icing Research Tunnel operating envelopes for large drop conditions at different airspeeds compared to Federal Aviation Administration (FAA) 14 CFR Parts 25 and 29, Appendix O. (a) 100 kn. (b) 250 kn. Freezing Drizzle (FZDZ). Freezing Rain (FZRA). Liquid water content (LWC).

Conclusion

The procedures and results of the full cloud calibration conducted in NASA Glenn's Icing Research Tunnel (IRT) from September 2023 to June 2024 have been described. The calibration came as a recommended practice from SAE's ARP5905 "Calibration and Acceptance of Icing Wind Tunnels" to perform a full calibration every 5 years. Uniform icing clouds were established with both the Mod1 and Standard nozzle sets and also large drop (LD) conditions. The median volumetric diameter (MVD) and liquid water content (LWC) curve fits for both nozzle sets have been established and shown to be within the ±10-percent targets for Federal Aviation Administration (FAA) 14 CFR Parts 25 and 29, Appendix C conditions (nozzle air pressure ≥10 psig) and within the target accuracy of ±20 percent for LD conditions (Mod1 nozzles with nozzle air pressure ≤8 psig).

A few changes were made to the IRT cloud calibration procedures, compared to those reported in 2019. The number of spraying Mod1 nozzles was adjusted from 103 to 101. The uppermost bins from the Optical Array Probe (OAP–230X; Particle Measuring Systems) were not used when there was larger scale probe data available. That is, the OAP–230X was used for drop diameters between 46 to 362 μm. Finally, the OAP-230X and OAP-230Y probes were calibrated with a spinning disk to measure the depth of field to better define the bins.

References

1. SAE International: Calibration and Acceptance of Icing Wind Tunnels. ARP5905, 2015.
2. Timko, Emily N., et al.: NASA Glenn Icing Research Tunnel: 2019 Cloud Calibration Procedures and Results. NASA/TM—20205009045, 2021. https://ntrs.nasa.gov
3. Federal Aviation Administration: Atmospheric Icing Conditions. U.S. Code of Federal Regulations, Title 14, Part 25, Appendix C, 2015.
4. Federal Aviation Administration: Supercooled Large Drop Icing Conditions. U.S. Code of Federal Regulations, Title 14, Part 25, Appendix O, 2015.
5. Ide, Robert. F.; and Sheldon, David W.: 2006 Icing Cloud Calibrations of the NASA Glenn Icing Research Tunnel. NASA/TM—2008-215177, 2008. https://ntrs.nasa.gov
6. Lilie, L.E.: Science Engineering Associates, Inc., Tolland, CT, email communication, 2024.
7. Federal Aviation Administration: Compliance of Transport Category Airplanes With Certification Requirements for Flight in Icing Conditions. Advisory Circular 25–28, 2014.
8. Science Engineering Associates, Inc.: WCM-2000. 2016. http://www.scieng.com/pdf/WCM2000User.pdf Accessed Sept. 21, 2023.
9. Steen, Laura-Cheri E.; Ide, Robert F.; and Van Zante, Judith F.: An Assessment of the Icing Blade and the SEA Multi-Element Sensor for Liquid Water Content Calibration of the NASA GRC Icing Research Tunnel. AIAA 2016–4051, 2016.
10. Rigby, David L.; Struk, Peter M.; and Bidwell, Colin: Simulation of Fluid Flow and Collection Efficiency for an SEA Multi-Element Probe. AIAA 2014–2752, 2014.
11. Struk, P.M.: NASA Glenn Research Center, Cleveland, OH, personal communication, 2014.